American Mineralogist, Volume 96, pages 599–608, 2011

A new thermodynamic analysis of the intergrowth of hedenbergite and magnetite with Ca-Fe-rich olivine

JIAWEN HU,[1,2,*] SHIDE MAO,[3] GUOQIANG DU,[4] YUNXIA WU,[1] AND PU ZHANG[1]

[1]College of Resources, Shijiazhuang University of Economics, Shijiazhuang 050031, Hebei, China
[2]State Key Laboratory of Ore Deposit Geochemistry, Institute of Geochemistry, Chinese Academy of Sciences, Guiyang 550002, Guizhou, China
[3]State Key Laboratory of Geological Processes and Mineral Resources, and School of Earth Sciences and Resources, China University of Geosciences, Beijing 100083, China
[4]Institute of Materials Science and Engineering, Shijiazhuang University of Economics, Shijiazhuang 050031, Hebei, China

ABSTRACT

Some errors and metastable phase relations are found in a recently reported oxygen fugacity–silica activity [logf_{O_2}-log$a$(SiO_2)] diagram of the fayalite-kirschsteinite-hedenbergite-magnetite-wollastonite (Fa-Kst-Hd-Mt-Wo) system at 400 °C and 1 kbar (Markl et al. 2001). Systematic thermodynamic analysis reveals that the composite exsolution lamellae of Mt and Hd in the olivine from the Ilimaussaq Intrusion, Greenland, should form when the reaction 3Fa+3Kst+O_2 = 3Hd+2Mt is overstepped on rapid cooling. This process is also accompanied by favorable f_{O_2} and a(SiO_2) conditions. It is also found that the reaction mechanisms from Ca-Fe-rich olivine (Fa+Kst) to Mt+Hd are very different above and below the equilibrium temperature of the Mt-absent reaction Hd+Kst = Fa+2Wo. The mechanisms above the equilibrium temperature are obviously simpler than those below the equilibrium temperature. Despite this difference, the two types of mechanisms have many features in common: (1) Mt and Hd can form in Ca-Fe-rich olivine on continuous cooling; (2) If a(SiO_2) is not buffered, an increase in f_{O_2} alone is enough to transform Ca-Fe-rich olivine into Mt and Hd; (3) At a fixed f_{O_2} or a(SiO_2), the formation of Mt and/or Hd on cooling requires appropriate a(SiO_2) or f_{O_2}; and (4) The increase in a(SiO_2) is favorable to the formation of Hd, but it is not essential for the intergrown exsolution of Mt and Hd. These common features are closely related to the fact that the process from Fa+Kst to Mt+Hd is an entropy decreasing oxidation reaction.

Keywords: Fayalite, kirschsteinite, hedenbergite, magnetite, exsolution, Schreinemakers analysis, oxygen fugacity, silica activity

INTRODUCTION

Magnetite and Ca-Fe-pyroxene (hedenbergite) exsolved from or intergrown with olivines have been found in a variety of geological settings, such as ultrahigh-pressure metamorphic rocks (Liu and Jin 2006; Liu et al. 2005; Zhang et al. 1999), mantle dunites (Ren et al. 2008), the Haladala gabbro intruding in Carboniferous volcanic strata (Xue 2008), a shallow-level Tertiary mafic intrusion (Ashworth and Chambers 2000), alkaline to peralkaline intrusion (Larsen 1976; Markl et al. 2001a), meteorites and planets (Krot et al. 1998a, 2000; Kurat et al. 2004; Mikouchi et al. 1995, 2000; Sautter et al. 2006; Zolensky et al. 2008), historic smelting slags (Lottermoser 2002), and burned coal waste piles (Cosca et al. 1989; Novikova 2009; Sokol et al. 2002).

Despite extensive studies in mineralogy, petrology, and geochemistry, systematic analysis of phase relations that are useful for analyzing the intergrowth conditions of magnetite, hedenbergite, and olivine is still scarce. Many years ago, Lindsley et al. (1968) and Guo and Wang (1988) made a detailed analysis of the phase relations of the Fe-O-SiO_2 system on the basis of Schreinemakers analysis and experimental results. Gustafson (1974) used qualitative T-f_{O_2} diagrams constructed from Schreinemakers analysis and experimental results to analyze the stability conditions of some phase assemblages including hedenbergite, andradite, H_2O and related minerals in the Fe-Ca-Si-O-H system, but his work did not include fayalite.

Krot et al. (1998a, 1998b) and Zolotov et al. (2006) made quantitative calculations and analysis of the thermodynamic behavior of mineral assemblages in the presence of aqueous solutions and coexisting gas. They also provided some phase diagrams at lower pressures and temperatures, such as a log[x(H_2O)/x(H_2)]-log[a(Fe^{2+})/a(Ca^{2+})] diagram at fixed log$a$(SiO_2) and temperature ($50 \le T \le 310$ °C) (Krot et al. 1998b), a T-log[x(H_2O)/x(H_2)] and T-log[a(Fe^{2+})/a(Ca^{2+})] diagram at fixed log$a$(SiO_2) and pressure (100 bar) (Krot et al. 1998a) and many other phase diagrams showing the influence of P, T, f_{H_2}/f_{H_2O}, f_{H_2}, water to rock ratio and phase composition on phase relations under different condition parameters (Zolotov et al. 2006).

Markl et al. (2001a) made a systematic thermodynamic calculation and analysis of the exsolution process of magnetite and hedenbergite in olivine samples from the augite syenite of the alkaline to peralkaline Ilimaussaq intrusion in South Greenland. The analysis involved five minerals: fayalite (Fa, Fe_2SiO_4), hedenbergite, (Hd, $CaFeSi_2O_6$), kirschsteinite (Kst, $CaFeSiO_4$), magnetite (Mt, Fe_3O_4), and wollastonite (Wo, $CaSiO_3$). In view of the heterogeneous exsolution from high-pressure mantle rocks

* E-mail: hu_jiawen@sina.com

to low-pressure meteorites, pressure was considered to be less important than T, f_{O_2}, and $a(SiO_2)$ (Markl et al. 2001a). Based on this consideration, Markl et al. (2001a) calculated the $\log f_{O_2}$-$\log a(SiO_2)$ diagram of the Fa-Hd-Mt-Wo system at 250, 400, 750, and 900 °C and an estimated pressure (1 kbar). The calculated $\log f_{O_2}$-$\log a(SiO_2)$ diagram did not include Kst, because they did not find thermodynamic data for Kst. To analyze the exsolution of Mt and Hd from olivine, the Kst-participating phase equilibria were incorporated into the $\log f_{O_2}$-$\log a(SiO_2)$ diagram at 400 °C and 1 kbar through Schreinemakers analysis and approximated estimation (Fig. 1). According to the calculated results, the primary olivines formed at T = 875 ± 15 °C and f_{O_2} between 1.2 and 2.3 log units below the QFM buffer. The $a(SiO_2)$ during the early stages of magmatic crystallization was below 0.4. On the other hand, the calculated olivine-clinopyroxene equilibria indicate temperatures between 300 and 750 °C at 1 kbar and f_{O_2} close to QFM for the exsolution process (Markl et al. 2001a, p. 43). The effect of temperature on the exsolution process is shown in Figure 2. According to Figures 1 and 2 and calculated T-f_{O_2}-$a(SiO_2)$ conditions, Markl et al. (2001a) concluded that the Fa+Kst assemblage may become unstable with respect to the Mt+Hd assemblage if both $a(SiO_2)$ and f_{O_2} stay constant, or if one or both of the two parameters increase. Composite exsolution lamellae were therefore considered to form during rapid cooling due to overstepping of the reaction Fa+Kst+1/3O_2 = Hd+2/3Mt.

However, several problems were found in the work of Markl et al. (2001a): (1) Figures 1 and 2 and some relevant reaction expressions are erroneous; (2) Figure 1 contains metastable phase relations; (3) Figures 1 and 2 were constructed for the exsolution of Mt and Hd at specified conditions, so they cannot be applied to other conditions, such as lower temperatures, or buffered f_{O_2} or $a(SiO_2)$. In particular, the influence of temperature on the phase behavior of the Fe-Ca-Si-O system is not represented explicitly in these phase diagrams. For example, Figure 1 is topologically equivalent to a binary phase diagram, in which a divariant assemblage only contains two phases, whereas a natural two-phase

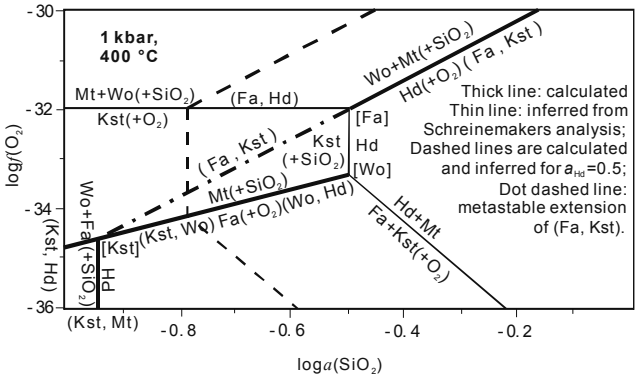

FIGURE 1. The $\log f_{O_2}$-$\log a(SiO_2)$ diagram of the Fe-Ca-Si-O system [after Fig. 9 of Markl et al. (2001a)]. To facilitate relevant analysis and discussion, the metastable extension of univariant curve (Fa, Kst) is added as dot/dash line. Also added are the labels for invariant point [Kst] and univariant curves (Kst, Hd), (Wo, Hd), (Fa, Hd), and (Fa, Kst). The SiO_2 and O_2 in parentheses denote the SiO_2 and O_2 components that are needed for the mass balance of their corresponding reactions (the same as in the figures below).

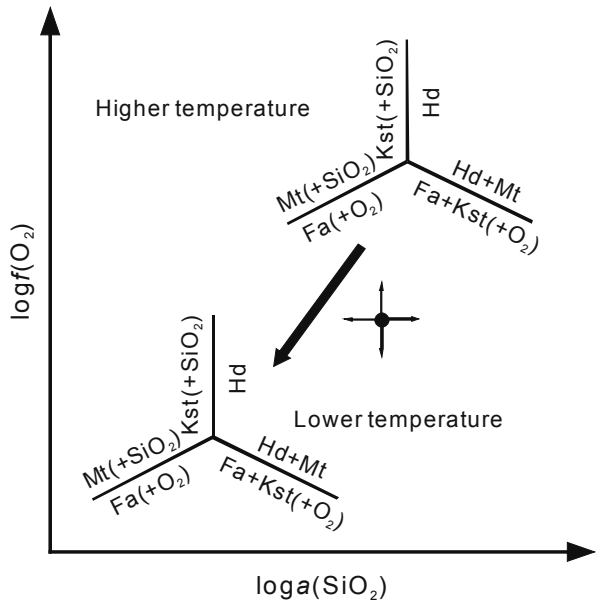

FIGURE 2. Schematic $\log f_{O_2}$-$\log a(SiO_2)$ diagram showing the temperature dependence of the invariant point [Wo] [from Fig. 10 of Markl et al. (2001a)]. The black dot indicates one of many possible f_{O_2}-$a(SiO_2)$ conditions under which the Fa-Kst solid solution at high temperatures would exsolve Mt+Hd during cooling.

assemblage may be multivariant, and a natural divariant assemblage approximated as the Fe-Ca-Si-O system may comprise three or more phases. For instance, according to the mineralogical phase rule (Korzhinskii 1959, 1966; Thompson 1970), the three-phase assemblages Fa+Mt+Hd, Fa+Hd+Kst, and Hd+Kst+Wo observed in natural and anthropogenic rocks, as well as some meteorites, are usually divariant or multivariant.

In view of the problems stated above and the frequent citation of the work of Markl et al. (2001a), it is necessary to remove the errors and metastable phase relations and modify some relevant conclusions. More importantly, the topological analyses and thermodynamic calculations mentioned above are only partially suitable for the analysis of the intergrowth conditions of Mt and Hd with olivine. For example, the topological analyses of Lindsley et al. (1968) and Guo and Wang (1988) did not contain Kst and Hd, whereas that of Gustafson (1974) did not include fayalite. The calculated results mentioned above do not include kirschsteinite. Furthermore, the $\log f_{O_2}$-$\log a(SiO_2)$ diagram is not valid at lower temperatures, which will be illustrated later. On the other hand, the quality of the data for Kst is still inadequate for reliable thermodynamic calculation. For these reasons, it is necessary to make a more complete thermodynamic analysis to obtain a better understanding of the phase behavior in natural rocks or petrologic experiments that are relevant to the Fe-Ca-Si-O system. For this purpose, a systematic thermodynamic and topological analysis is made by using a series of different phase diagrams constructed from Schreinemakers analysis and necessary thermodynamic constraints. Like the analysis of Markl et al. (2001a), the minerals in this work are confined to the Fa-Kst-Hd-Mt-Wo assemblage, because it captures many compatible assemblages associated with Mt, Hd, and Ca-Fe-rich olivine.

CORRECTION OF ERRORS IN THE WORK OF MARKL ET AL. (2001A)

Establishment of model system

Before discussing the phase relations of minerals, we need to use the extended Gibbs phase rule:

$$f = c - p + 2 - r \quad (1)$$

where f is the number of the degrees of freedom of a system, p and c are the numbers of phases and independent components in the system, respectively, and r is the number of independent constraints on intensive variables. The constraints exclude those with respect to compositions, concentrations, or partial pressures that arise from any stoichiometric relations (including charge-balance conditions), because these constraints have been counted in the definition of c (Hillert 2008, p. 157).

For the $\log f_{O_2}$-$\log a(SiO_2)$ diagram of the Fe-Ca-Si-O system at 400 °C and 1 kbar, $c = 4$, $r = 2$, where 2 denotes the constraints of fixed T and P. In this situation, we have

$$f = 4 - p + 2 - 2 = 4 - p \quad (2)$$

in which there are four phases in every invariant assemblage, and three phases in every univariant assemblage. That is, the phase relations in a quaternary system are topologically equivalent to those in a binary system. In this example, the coordinate variables f_{O_2} and $a(SiO_2)$ are essentially the external conditions of the minerals. As such, O_2 and SiO_2 are treated as external components in a theoretical analysis, and can be excluded from a chemography by projecting the quaternary phase composition space from O_2 and SiO_2 onto the Ca-Fe (or CaO-FeO) bar. The projection results are given in Figure 3, which is essentially the chemographic diagram of a model system. Subsequent to this treatment, all univariant reactions can be balanced in terms of Ca and Fe at first, and then in terms of O_2 and SiO_2. As done by Markl et al. (2001a), all phase assemblages or topological elements in this work are labeled with their absent phases. For example, the invariant assemblage or point from which phase Fa or Wo is absent is recorded as [Fa] or [Wo]. Similarly, the univariant assemblage or curve from which Fa and Wo are absent can be designated as (Fa, Wo).

Correction of reaction expressions

In this process, we found some errors in the following reactions: (1) The reaction $Kst+O_2 \leftrightarrow Mt+Wo+SiO_2$ along the univariant line (Fa, Hd) in Figure 1 should be $Kst+O_2 \leftrightarrow Mt+Wo$ (i.e., $6Kst+O_2 = 2Mt+6Wo$). The slope of (Fa, Hd) should be zero, which is consistent with the real result. (2) The reaction on the line $Fa+O_2 \leftrightarrow Mt+SiO_2$ should be $3Fa+O_2 = 2Mt+3SiO_2$, not $Fa+0.5O_2 = Mt+SiO_2$ [namely reaction 3 of Markl et al. (2001a)]. (3) The "univariant reaction" on the line marked as $Fa+Kst+O_2 \leftrightarrow Mt+Hd$ is incorrect. As computed above, a univariant assemblage in the quaternary system at constant T and P only contains three participating phases, whereas the "univariant reaction" $Fa+Kst+O_2 \leftrightarrow Mt+Hd$ has four participating phases, which is obviously not permitted by the phase rule. In fact, the reaction $Fa+Kst+O_2 \leftrightarrow Mt+Hd$ should be regarded as a univariant reaction occurring in a ternary model system (Fe-Ca-Si) at fixed P or T. It is a linear combination of the following two degenerate univariant reactions in the Fe-Ca model system:

(Wo, Kst): $3Fa+O_2 = 2Mt+3SiO_2$
(Wo, Mt): $Kst+SiO_2 = Hd$

For this reason, the line $Fa+Kst+O_2 \leftrightarrow Mt+Hd$ should be removed and replaced with lines (Wo, Kst) and (Wo, Mt). Consequently, there should be four univariant lines about invariant point [Wo]. Nevertheless, the equilibrium line of ternary univariant reaction $Fa+Kst+O_2 \leftrightarrow Mt+Hd$ at fixed P or T can also be projected on the $\log f_{O_2}$-$\log a(SiO_2)$ diagram of the binary model system. If so, the projection should be parallel to the $\log a(SiO_2)$ axis, and each point on it should correspond to a different temperature or pressure.

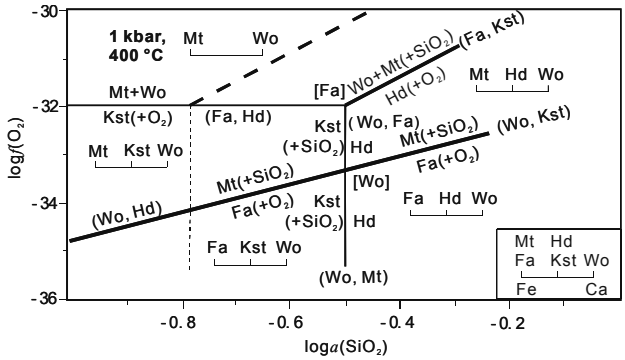

FIGURE 3. Corrected $\log f_{O_2}$-$\log a(SiO_2)$ diagram of the Fe-Ca-Si-O system at 400 °C and 1 kbar. The insertion in the bottom corner is the projection of the chemographic diagram of the Fe-Ca-Si-O system from O_2 and SiO_2.

Correction of univariant curves

The correct topology of the four curves about [Wo] (Fig. 3) is derived using Schreinemakers' rules (Schreinemakers 1915–1925). Figure 3 shows that the univariant curves (Wo, Hd) and (Wo, Kst) about [Wo] degenerate into one curve. They can be arranged like non-degenerate curves (Usdansky 1983; Zen 1966). As a result, the stable and metastable parts of (Wo, Hd) overlap the metastable and stable parts of (Wo, Kst), respectively. Similar degeneration also occurs for (Wo, Fa) and (Wo, Mt) in Figure 3, as well as (Kst, Wo) and (Kst, Hd) in Figure 1. Such degeneration is a natural result of Schreinemakers analysis, where the topological arrangements of [Wo] and [Fa] correspond to cases B and D of Figures 16 and 17 of Zen (1966). The univariant curve $Fa+Kst+O_2 \leftrightarrow Mt+Hd$ inferred for $a_{Hd} = 0.5$ (plotted with dashed lines) in Figure 1 has been corrected in the same way (Fig. 3). In contrast to Figure 1, Figure 3 has a sector bounded by (Wo, Mt) and (Wo, Kst), which leaves room for the assemblages Fa+Hd and Hd+Wo. In fact, Fa+Hd and Hd+Wo have been found in historical smelting slags (Lottermoser 2002) and Allende dark inclusions (Krot et al. 1998a; Zolensky et al. 2008).

Elimination of metastable phase relations

As indicated by the dotted and dashed line in Figure 1, the invariant point [Kst] lies on the metastable part of non-degenerate

curve (Fa, Kst) radiating from [Fa]. According to the stability theory of invariant points (Cheng and Greenwood 1990; Hu et al. 2000; Lépine et al. 1992; Vielzeuf and Boivin 1984), [Kst] should be metastable. Similarly, [Kst] also lies on the metastable part of degenerate curve (Wo, Kst), so it is still metastable. That is, the curves radiating from [Kst] are all metastable, so they should be removed from the diagram. The stable topology of the system is presented in Figure 3. To be consistent with Figure 3, the topology about [Wo] in Figure 2 should also be corrected to that shown in Figure 4.

THERMODYNAMIC ANALYSIS BASED ON PHASE DIAGRAM TOPOLOGY

The logf_{O_2}-log$a$(SiO_2) diagram at 400 °C and 1 kbar

The stability field of Kst is bounded by reactions $6Kst+O_2 = 2Mt+6Wo$ and $Kst+SiO_2 = Hd$. This suggests that Kst is only stable at low $a(SiO_2)$ and low to intermediate f_{O_2}. At higher f_{O_2}, Fa+Kst tends to transform into Mt+Wo. At higher $a(SiO_2)$, Fa+Kst tends to transform into Fa+Hd, rather than Mt+Hd. These results are consistent with many observations, whereas the latter conclusion cannot be drawn from the logf_{O_2}-log$a(SiO_2)$ diagram of Markl et al. (2001a).

The intergrowth mechanisms of the Hd, Mt, and Fe-rich olivine are obviously more complex. If an increase in f_{O_2} gives rise to reaction $Fa+O_2 = Mt+SiO_2$, the resulting SiO_2 may be enough to start reaction $Kst+SiO_2 = Hd$. The direct and indirect effects of increasing f_{O_2} give rise to the simultaneous exsolution of Hd and Mt. If there is an increase in $a(SiO_2)$ caused by other factors, it will favor the formation of Hd, but it is obviously not indispensable for the intergrown exsolution of Hd and Mt. This conclusion is different from that of Markl et al. (2001a). Moseley (1984) found that some Type A symplectites in olivine (consisting of Ca-rich pyroxene and magnetite) have magnetite cores. This suggests that magnetite may be the first phase to precipitate. The

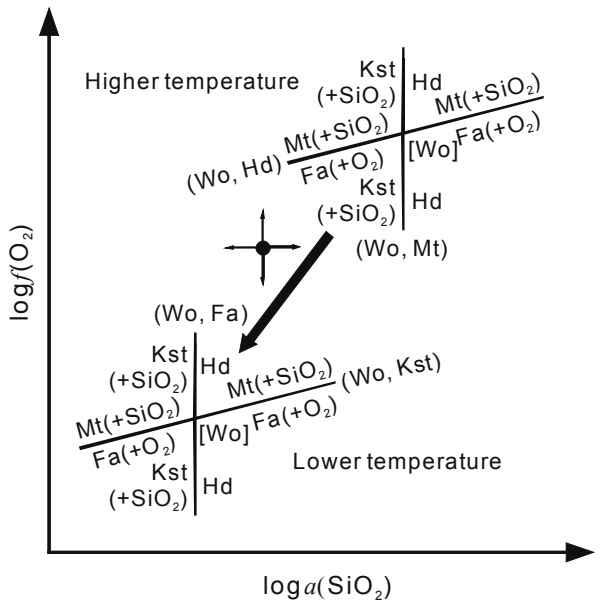

FIGURE 4. Corrected form of the schematic logf_{O_2}-log$a(SiO_2)$ diagram showing the temperature dependence of invariant point [Wo].

average volume ratio of Ca-rich pyroxene and magnetite is about that observed in electron micrographs. Similar results were also found in the symplectic exsolution in olivine from the Nakhla Martian meteorite (Mikouchi et al. 2000). Furthermore, many electron micrographs indicate that Ca-rich pyroxene continued to grow after magnetite formation had ceased (Moseley 1984). That is, the reaction $Kst+SiO_2 = Hd$ can proceed independent of the oxidation of fayalite.

Of course, the influence of temperature on the exsolution of Hd and/or Mt cannot be explained by Figure 3 alone. According to Figure 8 of Markl et al. (2001a), the reactions $Kst+SiO_2 = Hd$ and $Fa+O_2 = Mt+SiO_2$ must be processes that decrease entropy. Therefore, if temperature continuously decreases, the two reaction equilibria will move toward the products (Hd and Mt), and their equilibrium curves will therefore move toward lower $a(SiO_2)$ and f_{O_2}, respectively. For this reason, even if $a(SiO_2)$ and f_{O_2} remain constant on cooling, the equilibrium curves of reactions $3Fa+O_2 = 2Mt+3SiO_2$ and $Kst+SiO_2 = Hd$ can also be overstepped if temperature decreases to a sufficiently low level. In this case, the Fa+Kst assemblage will become unstable with respect to the Mt+Hd assemblage.

For Ca-Fe-rich olivine in a specified environment, there may be multiple factors that are favorable to the exsolution of Hd and Mt, such as the assimilation of quartz-bearing (or SiO_2-bearing) wall rocks, base rocks or melts (Markl et al. 2001a), or the internal changes buffered by local mineral assemblage (Bowen and Schairer 1935; Markl et al. 2001b), or the participation of oxidizing fluids (Lottermoser 2002; Markl et al. 2001a; Sokol et al. 2002), or the supply of O_2 from a late-stage residual melt (Morse 1980, p. 717), or the high Fe^{3+} content of magmatic minerals (Markl et al. 2001a). In these cases, $a(SiO_2)$ and f_{O_2} may increase simultaneously to a level that is high enough for Hd and Mt to form in (or exsolve from) the host olivine even if T and P remain constant.

The isobaric T-logf_{O_2} and T-log$f(SiO_2)$ diagrams

Considering the importance of T, f_{O_2}, and $a(SiO_2)$, we construct isobaric T-logf_{O_2} and T-log$a(SiO_2)$ diagrams as the basis of our analysis. The corresponding chemographic diagram can be obtained by projecting the quaternary phase composition space from O_2 or SiO_2 onto the Fe-Ca-Si or Fe-Ca-O plane. With this projection, all univariant assemblages in the ternary model system (Fe-Ca-Si or Fe-Ca-O) can be determined. In the isobaric T-logf_{O_2} or T-log$a(SiO_2)$ diagram, the arrangement of univariant curves is based on Schreinemakers' rules and the assumption that every reactant or product assemblage including O_2 or SiO_2 should lie on the higher temperature and lower f_{O_2} or $a(SiO_2)$ side. The results are given in Figures 5 and 6.

In Figure 5, the chemographic diagram clearly shows a compositional coincidence of two phases and a colinearity of three phases. Because of the unusual compositional degeneracy, the phase relations in Figure 5 are highly simplified, where the magnetite is absolutely indifferent to all univariant reactions in the binary subsystem, so it may be present throughout the diagram. The results are completely consistent with the general Schreinemakers analysis of Zen (1966; case E of Fig. 21, p. 39). According to Figure 5, the Fa+Wo (or Fa+Wo+Mt) assemblage is only stable at lower temperatures. This result is consistent

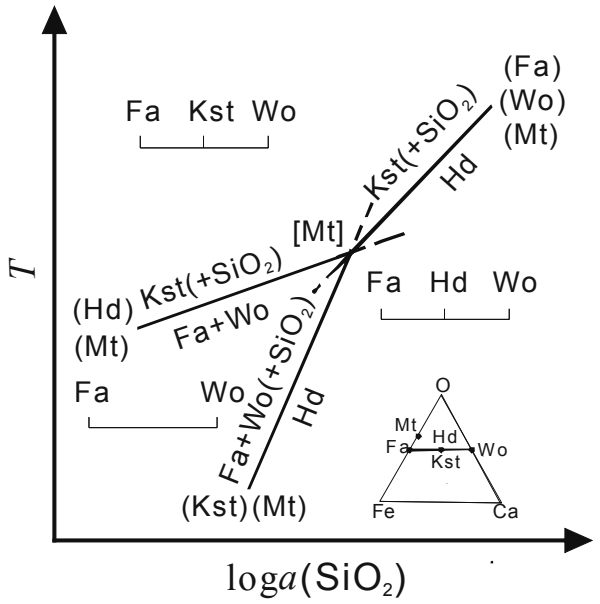

FIGURE 5. The isobaric T-log$a$(SiO_2) diagram of the Fe-Ca-Si-O system. Note that magnetite (Mt) is absent from all reactions in the diagram.

with Figure 6. Despite the unusual degeneracy, Figure 5 is still able to give some useful information. For example, the Fa+Hd (or Fa+Hd+Mt) assemblage can form from Ca-Fe-rich olivine (Fa+Kst) with decreasing temperature and/or increasing $a(SiO_2)$, but the paths are very different at temperatures above and below the invariant point.

More information on the stability conditions and compatibility relations of minerals can be obtained from Figure 6. The compatibility diagrams indicate that Mt, Fa, and Hd are chemographically exterior phases for the silica-undersaturated system, so the two-phase assemblages Mt+Fa and Fa+Hd can be present in all sectors of the diagram if only the system has an appropriate bulk composition (Stout and Guo 1994). This suggests that Hd and/or Mt can form in (or exsolve from) Ca-rich Fe-Mg olivine in a very wide T-f_{O_2} range.

(1) The conditions of separate intergrowth of Hd or Mt with Fe-rich olivine. As seen in Figure 6, the separate occurrence of Hd or Mt can be found in most sectors. The only exception is the sector between (Fa) and (Kst), where Hd and Mt only occur in the same divariant assemblage (Hd+Mt+Fa or Hd+Mt+Wo). Many assemblages containing Hd or Mt have close relationships to specified thermodynamic conditions. For example, all divariant assemblages including Fa+Kst (namely Fa+Kst+Hd/Wo/Mt) fall in the low f_{O_2} region, where Fa+Kst+Hd and Fa+Kst+Wo are also indicative of high and low temperatures, respectively. For example, the Fa+Kst+Hd and Fa+Kst+Mt assemblages observed in veined basic melt-rocks in burned spoil-heaps have been estimated to form at f_{O_2} of 0.6–0.9 below FMQ and T = 1050–1100 °C (Sokol et al. 2002). The Fa+Kst+Wo assemblage in the sector between (Mt) and (Hd) suggests that the Fa+Kst assemblage can occur at very low T and f_{O_2}. This is confirmed by the coexistence of both fayalitic and kirschsteinitic olivines found in the same smelting slag pots in north Queensland (Lottermoser 2002). The Fa+Hd+Wo assemblage is characterized by low temperature and low- to intermediate-f_{O_2} conditions. This is evidenced by the appearance of minor Wo in some olivine-pyroxene (Hd) historical smelting slags in Montalbion (Lottermoser 2002). The Fa+Kst+Hd and Hd+Kst+Wo assemblages are only stable at high temperatures, where the Fa+Kst+Hd assemblage is indicative of high-temperature and low-f_{O_2} conditions. For example, the Hd+Kst+Wo assemblage found in Allende dark inclusions (Krot et al. 1998a; Zolensky et al. 2008) should form at high temperatures. In fact, many mineralogical and geochemical features in the inclusions point to thermal metamorphism after aqueous alternation (Krot et al. 1998a; Zolensky et al. 2008). The temperature of the metamorphism may be high up to 700–1000 °C (Brenker and Krot 2004; Buchanan et al. 1997; Kojima and Tomeoka 1996; Krot et al. 1997). Like Hd+Kst+Fa/Wo, Hd+Kst is also indicative of high temperatures. This is consistent with the assemblage Hd+Kst+Ca-rich olivine found in the D'Orbigny angrite, which is thought to have been produced at about 1000 °C (Kurat et al. 2004).

(2) The conditions of simultaneous intergrowth of Hd and Mt with Fe-rich olivine. The Mt+Hd assemblage can occur in two adjacent sectors separated by (Fa). Consequently, Mt+Hd can exist stably at both high and low temperatures if f_{O_2} is high enough.

The two sectors also imply two possible paths for the formation or exsolution of Mt+Hd: (1) Reaction (Wo), or reaction (Wo) plus reaction (Fa). That is, Hd and Mt can be produced from Fa+Kst during cooling and/or an increase in f_{O_2}. This is a simpler explanation of the first two mechanisms mentioned above. Nevertheless, this path is only applicable above the equilibrium temperature of reaction (Mt). Considering the increase in relative f_{O_2} due to cooling and the increase in absolute f_{O_2} caused by the influx of hydrous fluids, the real exsolution mechanisms of Hd and Mt in the olivine from the Ilimaussaq Intrusion must have experienced reaction (Wo). The reaction Kst+SiO_2 = Hd could

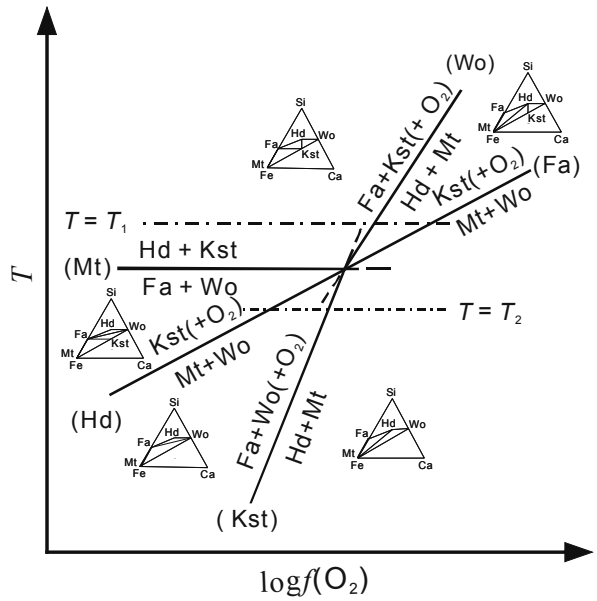

FIGURE 6. The isobaric T-logf_{O_2} diagram of the Fe-Ca-Si-O system. The dot/dash lines are the projections of two binary reaction equilibrium curves in logf_{O_2}-log$a$(SiO_2) space at constant pressure and temperature.

have occurred as well in some local environments contaminated by SiO_2-rich lavas, wall rocks or base rocks, or occurred under suitable T-f_{O_2} conditions for silica-producing reactions (Markl et al. 2001a, 2001b).

(2) Reaction (Hd) plus reaction (Kst). Mt+Hd can be produced from Fa and Kst through these two reactions (not one of them) during cooling and/or the increase in f_{O_2}. Apparently, this path is only applicable below the equilibrium temperature of reaction (Mt). According to the mineralogical and petrological features and natural conditions, Fa+Mt+Hd should be a major mineral assemblage in most of the smelting slags in north Queensland (Lottermoser 2002). This assemblage should result from late weathering and oxidation at ambient temperatures. In addition, there is considerable evidence indicating that the intergrowth of Mt, Hd, and Fa in chondrites and dark inclusions in some meteorites formed at low temperatures (Krot et al. 1998a, 1998b; Zolensky et al. 2008; Zolotov et al. 2006). The assemblage formed by initial oxidation of metal to magnetite and subsequent replacement of Mt by Fa and Hd at lower temperatures (below 350 °C) in the presence of reducing materials (Fe-bearing metals and troilite) and SiO_2-bearing aqueous solutions, where some grains of Fa and Hd would have formed by direct deposition from aqueous solutions containing Fe^{2+} and Ca^{2+} and SiO_2 (Krot et al. 2000).

The isothermal and isobaric logf_{O_2}-log$a$(SiO_2) diagram at lower temperatures

In Figure 6, the intersection of isotherm $T = T_1$ with (Wo) and (Fa) forms isothermal and isobaric invariant points [Wo] and [Fa]. The phase relations about [Wo] and [Fa] at T_1 = 400 °C and P = 1 kbar are shown in Figure 3, where Fa+Wo is metastable. The lower isotherm $T = T_2$ intersects (Hd) and (Kst) at isothermal and isobaric invariant points [Hd] and [Kst]. The stable phase relations about [Hd] and [Kst] are presented in Figure 7, where Hd+Kst is metastable.

This diagram may be used for the thermodynamic analysis of mineral assemblages at temperatures below the equilibrium temperature of reaction (Mt) in Figure 6. As is evident in Figure 7, only fayalite can stably coexist with the Hd+Wo assemblage. This suggests that the olivine intergrown with Hd and Wo found in the historical smelting slags in north Queensland (Lottermoser 2002) must be fayalite, rather than Kst. On the other hand, the metastability of Hd+Kst at low temperatures also strongly supports a high-temperature formation mechanism of the Hd+Kst+Wo assemblage in Allende dark inclusions (Krot et al. 1998a; Zolensky et al. 2008). This is consistent with many mineralogical and geochemical features (Brenker and Krot 2004; Buchanan et al. 1997; Kojima and Tomeoka 1996; Krot et al. 1997, 1998a; Zolensky et al. 2008).

According to Figure 7, if f_{O_2} increases continuously, the Fa+Kst assemblage will evolve into Mt+Kst and Mt+Wo in sequence. In this process, the SiO_2 produced from oxidation reactions may be enough to start the reaction $2Mt+6Wo+6SiO_2 = 6Hd+O_2$. If so, Mt+Wo will be transformed into Mt+Hd. The overall effect of this process is that an increase in f_{O_2} alone can cause a transformation from Fa+Kst to Mt+Hd. Of course, if there is an increase in $a(SiO_2)$ independent of the oxidation process, it will be favorable to the formation of Hd, but it is not essential for the transformation of Fa+Kst toward Mt and Hd. These conclusions are very similar to those drawn from Figure 3, but the reaction mechanisms are very different.

The T-logf_{O_2} diagram at constant P and a(SiO_2) and T-log$a$(SiO_2) diagram at constant P and f_{O_2}

In mineralogical and petrological processes, there are often circumstances in which the chemical potential (or activity, fugacity, composition, concentration, etc.) of a component is buffered or controlled by some thermodynamic processes or assemblages of species or phases in the immediate surroundings. This possibility necessitates the construction of phase diagrams at fixed chemical potential (or a relevant property of the component). For the Fe-Ca-Si-O system in this work, we only consider the T-logf_{O_2} diagram at constant P and $a(SiO_2)$ and the T-log$a(SiO_2)$ diagram at constant P and f_{O_2}. In these diagrams, both f_{O_2} and $a(SiO_2)$ are the condition parameters external to the mineral assemblages. For this reason, O_2 and SiO_2 should be treated as external components, so they should be excluded from the phase compositions by chemographic projections. In this way, we can obtain a binary model system, whose chemographic diagram is a Fe-Ca bar. The phase diagram topology can be constructed with Schreinemakers' rules under necessary constraints. Of course, these constraints must include those used in the construction of Figures 5 and 6. In addition, the following constraints embodied in Figures 3 and 7 must also be satisfied: (1) In Figures 8a and 9a, the metastable extensions of (Fa, Kst) and (Wo, Kst) intersect each other, and the metastable extensions of (Fa, Hd) and (Wo, Hd) intersect each other. The intersections are the metastable invariant points [Kst] and [Hd] (not shown). (2) In Figure 8b, the metastable extensions of (Hd, Fa) and (Kst, Fa) intersect at metastable invariant point [Fa] (not shown) in the divariant Fa+Wo region between [Hd] and [Kst]. In Figure 9b,

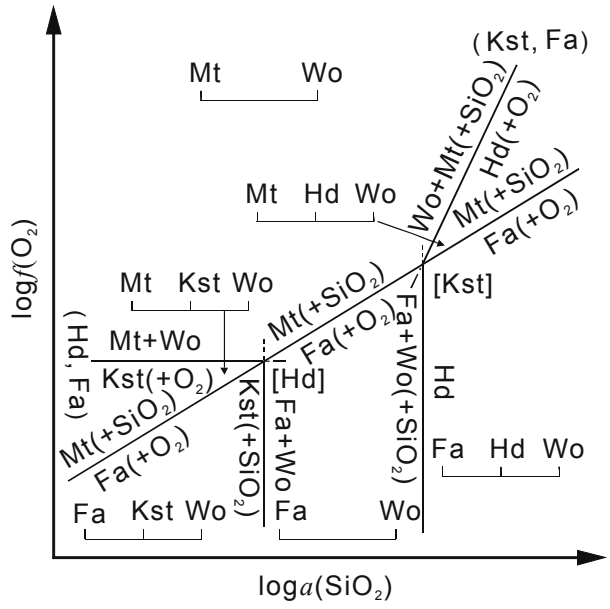

FIGURE 7. The isobaric logf_{O_2}-log$a$(SiO_2) diagram of the Fe-Ca-Si-O system at a lower temperature [below the magnetite absent reaction equilibrium curve (Mt)].

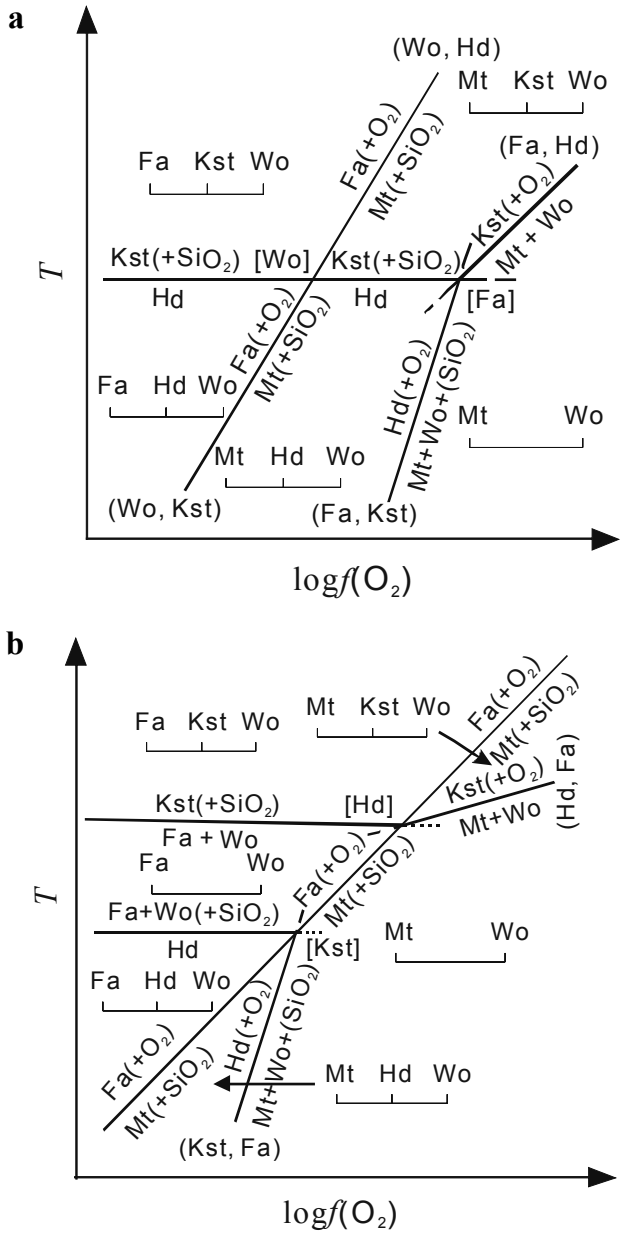

FIGURE 8. The T-logf_{O_2} diagram of the Fe-Ca-Si-O system at constant P and $a(SiO_2)$. (**a**) and (**b**) are stable at different silica activities.

the metastable extensions of (Mt, Fa), (Hd, Fa), and (Kst, Fa) intersect at a point in the divariant Fa+Wo region enclosed by the [Mt]-[Hd]-[Kst] triangle.

By simple analysis of Figures 8 and 9, the following conclusions can be obtained: (1) the Fa+Kst assemblage at fixed $a(SiO_2)$ or f_{O_2} can evolve into Mt+Hd on cooling if the system has an appropriate f_{O_2} or $a(SiO_2)$; (2) an increase in $a(SiO_2)$ alone can transform Kst to Hd, but it cannot transform Fa+Kst into Mt+Hd; and (3) at fixed $a(SiO_2)$, an increase in f_{O_2} alone may be enough to transform Fa into Mt, but it cannot transform Fa+Kst into Mt+Hd. This is because the SiO_2 produced in oxidation reactions is consumed by the $a(SiO_2)$ buffering system so that $a(SiO_2)$ remains at a fixed level. This is very different from the conclusions drawn from Figures 3 and 7.

DISCUSSION

Preliminary calculation of phase equilibria involving kirschsteinite

Davidson and Mukhopadhyay (1984) inferred a temperature function of apparent standard Gibbs free energy for Kst [μ^0(Kst)]. At 298 K, its value relative to oxides is –102.79 ± 0.8 kJ/mol. They also obtained a standard free energy relation for the ion-exchange equilibrium between four olivine end-members: F^0 = 2[μ^0(Mo) – μ^0(Kst)]+ μ^0(Fa) – μ^0(Fo) = 12.66 ± 1.6 kJ, where Mo and Fo are monticellite and forsterite, respectively. In the work of Hirschmann (1991), the F^0 value was modified as 9.5 ± 1.0 kJ/mol. Davidson and Lindsley (1989) gave a modified free energy expression for Kst, which is a function of both temperature and pressure, where the 298.15 K value of μ^0(Kst) relative to oxides is refined as –87.452 kJ/mol. In the data file of software QUILF (Andersen et al. 1993), the μ^0(Kst) at 298.15 K is –1799.164 kJ/mol. According to the data of QUILF, the F^0 should be 9.8 kJ. The phase diagrams calculated with the above data for Kst and those of relevant minerals from the databases of Holland and Powell (1998), Berman (1988), and Berman and Aranovich (1996) confirm the topological configuration in Figure 3, as well as those in other figures (e.g., Figs. 5, 8, and 9). Meanwhile, we also found some problems associated with the quality of the data or models for Kst and/or relevant minerals. For example, the database of QUILF or its relevant models, is obviously inconsistent with those of Holland and Powell (1998), Berman (1988), and Berman and Aranovich (1996). For the standard free energies of minerals closely relevant to the derivation of the data of Kst, the biggest difference is up to 12.281–14.553 kJ/mol. When the above data for Kst are used together with the database of Holland and Powell (1998), the calculated logf_{O_2}-log$a(SiO_2)$ diagram at 400 °C and 1 kbar has the same topology as Figure 3, but the equilibrium lines of reactions 2Mt+6Wo = 6Kst+O_2 and Kst+SiO_2 = Hd lie at logf_{O_2} = –33.281 and log$a(SiO_2)$ = –1.855, respectively, where the $a(SiO_2)$ is much lower than the value estimated by Markl et al. (2001a). Similar results can be obtained if the data of relevant minerals are replaced with those of Berman (1988) and Berman and Aranovich (1996). In addition, calculated results for the phase equilibria in Figures 6 and 7 also indicate that the data of Kst and relevant models are still inadequate, so they should be refined and constrained with extensive experimental data (Bowen et al. 1933a, 1933b; Brown 1982; Davidson and Mukhopadhyay 1984; Gustafson 1974; Johnson and Muan 1967; Kawasaki 1998a, 1998b, 1999, 2001; Mukhopadhyay and Lindsley 1983; Selleby 1997).

The possibility of ferroakermanite at lower temperatures

According to the experiments of Bowen et al. (1933b) (p. 211–212), the Wo+Kst assemblage buffered by metallic iron forms ferroakermanite (Fe-Ak, $Ca_2FeSi_2O_7$) below 775 ± 25 °C at atmospheric pressure. This result indicates that the change in entropy ($\Delta_r S$) in the reaction Kst+Wo = Fe-Ak is negative. In the high-pressure hydrothermal experiments of Gustafson (1974), the assemblage Kst+Wo was synthesized from oxide mixtures over a wide temperature range (T < 1000 °C) under reducing conditions, but Fe-Ak was not encountered. Gustafson (1974) also made a series of experimental runs of oxides with a

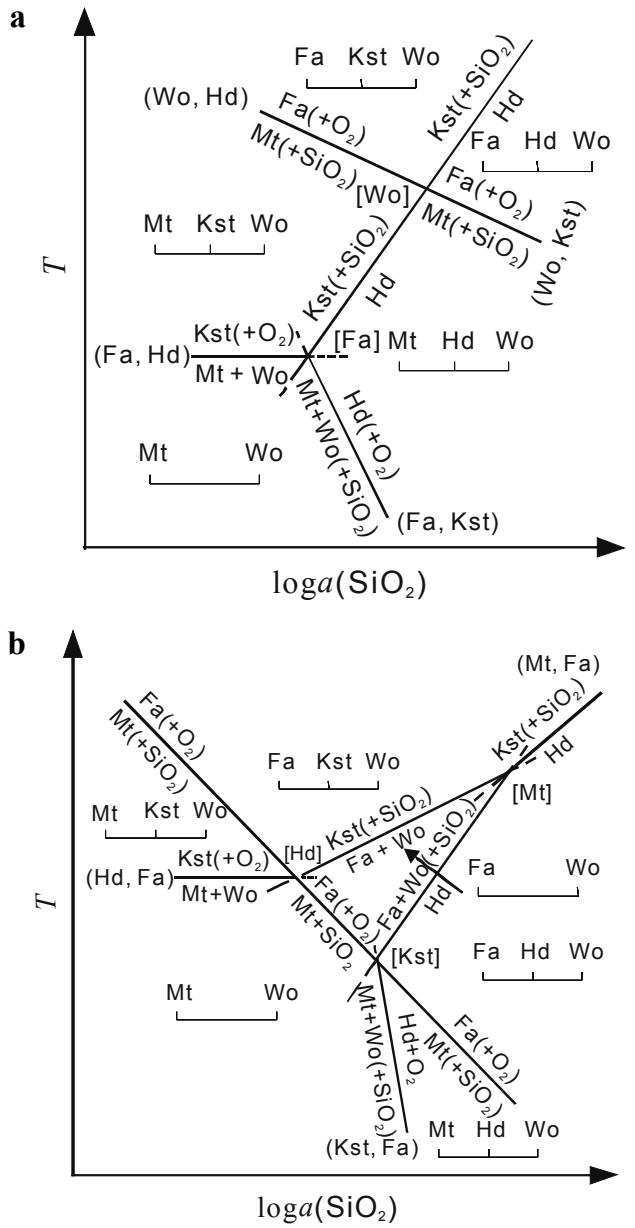

Figure 9. The T-log$a$(SiO_2) diagram of the Fe-Ca-Si-O system at constant P and f_{O_2}. (**a**) At f_{O_2} above the invariant point in Figure 6; (**b**) at f_{O_2} below the invariant point in Figure 6.

Fe-Ak bulk composition at P = 2000 bar, T = 433–658 °C, and f_{O_2} buffered by iron-magnetite (IM), iron-quartz-fayalite (IQF), or fayalite-magnetite-quartz (FMQ). Similarly, ferroakermanite was not detected, but the Wo+Kst assemblage formed at f_{O_2} buffered by IM or IQF. Providing that these results are correct, the equilibrium temperatures of the reaction Kst+Wo = Fe-Ak (if any) at higher pressures must be lower than the experimental temperatures, i.e., the equilibrium P-T curve of the reaction Wo+Kst = Fe-Ak must have a negative slope:

$$\left(\frac{\partial P}{\partial T}\right)_{\Delta_r G=0} = \frac{\Delta_r S}{\Delta_r V} < 0 \cdot \quad (3)$$

Accordingly, the equilibrium temperature of the reaction at the calculated pressure of Figure 1 should be obviously lower than 775 ± 25 °C. On the other hand, Figures 6, 8, and 9 indicate that Kst may be oxidized into Mt+Wo at lower temperatures, even if f_{O_2} is very low. This is supported by experimental results (Gustafson 1974). After the redox reaction, the free energy of the system should drop greatly. That is, Mt+Wo is likely to be more stable than Fe-Ak at lower temperatures. Furthermore, the Kst+Wo assemblage may also change into Hd+Wo or Fa+Wo through the reaction Kst+SiO_2 = Hd or 2Kst+SiO_2 = Fa+2Wo at lower temperatures and/or high a(SiO_2) (Figs. 3, 5, and 7–9). In addition, the low silica content of Fe-Ak indicates that Fe-Ak may be metastable at high a(SiO_2). These factors may help to explain the rarity of Fe-Ak in experimental or natural mineral assemblages.

So far, the stability conditions of Fe-Ak remain unclear. The possibility for the presence of Fe-Ak at lower temperatures has not been convincingly confirmed or excluded by field observations or experiments. If the reaction Wo+Kst = Fe-Ak does exist under certain P-T-f_{O_2}-a(SiO_2), the Wo+Kst assemblage will be replaced with Fe-Ak+Wo or Fe-Ak+Wo. In this case, the phase diagram topology must include additional invariant point(s).

Concluding Remarks

Several errors are found in the logf_{O_2}-log$a$(SiO_2) diagram and relevant reactions of the Fe-Ca-Si-O system at 400 °C and 1 kbar obtained by Markl et al. (2001a). The "univariant reaction" Fa+Kst+1/3O_2 = Hd+2/3Mt is actually a linear combination of two degenerate univariant reactions, i.e., Fa+1/3O_2 = 2/3Mt+SiO_2 and Kst+SiO_2 = Hd. Consequently, the corresponding "univariant curve" should be replaced with two univariant curves. The Kst-absent invariant point in the logf_{O_2}-log$a$(SiO_2) diagram is metastable, so it should be removed. According to the corrected logf_{O_2}-log$a$(SiO_2) diagram at 400 °C and 1 kbar, an increase in silica activity alone cannot lead to the intergrown exsolution of Mt and Hd from Ca-Fe-rich olivine. The composite exsolution lamellae of Mt and Hd in the olivine samples from the Ilimaussaq Intrusion should form when the reaction 3Fa+3Kst+O_2 = 3Hd+2Mt is overstepped on rapid cooling. The exsolution process is also accompanied by favorable f_{O_2} and a(SiO_2) conditions, namely increases in O_2 fugacity and silica activity.

It is found that the explanation of Markl et al. (2001a) based on the logf_{O_2}-log$a$(SiO_2) diagrams cannot be applied to low temperatures, because the reaction mechanisms from Ca-Fe-rich olivine (Fa+Kst) to Mt+Hd are very different above and below the equilibrium temperature of the reaction (Mt). Above this temperature, the process can be realized through reaction 3Fa+3Kst+O_2 = 3Hd+2Mt (or two equivalent reactions Fa+1/3O_2 = 2/3Mt+SiO_2 and Kst+SiO_2 = Hd). Below this temperature, the process can be realized through reactions 6Kst+O_2 = 2Mt+6Wo and 6Fa+6Wo+O_2 = 6Hd+2Mt, or some simpler reactions that are equivalent to them.

Despite the great difference in reaction path, the two types of mechanisms have some features in common: (1) Mt and Hd can form in (or exsolve from) Ca-rich Fe-Mg olivine on continuous cooling; (2) if a(SiO_2) is not buffered, an increase in f_{O_2} alone is enough to initiate the reaction from Ca-Fe-rich olivine to Mt and Hd over a wide range of temperature; (3) at a fixed f_{O_2} or a(SiO_2), the formation of Mt and/or Hd on cooling requires appropriate

$a(SiO_2)$ or f_{O_2}; and (4) an increase in silica activity is favorable to the formation of Hd, but it is not essential for the intergrown exsolution of Mt and Hd from Ca-Fe-rich olivine. These common features are determined by such a fact that the process from Fa+Kst to Mt+Hd is an entropy-decreasing oxidation reaction, whose direction is mainly determined by temperature and f_{O_2} if the change in pressure is not very large.

ACKNOWLEDGMENTS

We are grateful to Donald H. Lindsley, Michail I. Petaev, and associate editor Rhian Jones for their constructive comments and suggestions. We thank Dimitrios Xirouchakis for helping us find the data for kirschsteinite. This work was supported by the National Natural Science Foundation of China (40873018), the Open Foundation of the State Key Laboratory of Ore Deposit Geochemistry, Institution of Geochemistry (Guiyang), Chinese Academy of Sciences (200807), the Natural Science Foundation of Hebei Province (D2008000535), and the Open Fund of the State Key Laboratory of Oil and Gas Reservoir Geology and Exploitation (PLC201001).

REFERENCES CITED

Andersen, D.J., Lindsley, D.H., and Davidson, P.M. (1993) QUILF: A PASCAL program to assess equilibria among Fe-Mg-Mn-Ti oxides, pyroxenes, olivine, and quartz. Computers and Geosciences, 19, 1333–1350.

Ashworth, J.R. and Chambers, A.D. (2000) Symplectic reaction in olivine and the controls of intergrowth spacing in symplectites. Journal of Petrology, 41, 285–304.

Berman, R.G. (1988) Internally-consistent thermodynamic data for minerals in the system Na_2O-K_2O-CaO-MgO-FeO-Fe_2O_3-Al_2O_3-SiO_2-TiO_2-H_2O-CO_2. Journal of Petrology, 29, 445–522.

Berman, R.G. and Aranovich, L.Y. (1996) Optimized standard state and solution properties of minerals I. Model calibration for olivine, orthopyroxene, cordierite, garnet, and ilmenite in the system FeO-MgO-CaO-Al_2O_3-TiO_2-SiO_2. Contributions to Mineralogy and Petrology, 126, 1–24.

Bowen, N.L. and Schairer, J.F. (1935) The system MgO-FeO-SiO_2. American Journal of Science, 29, 151–217.

Bowen, N.L., Schairer, J.F., and Posnjak, E. (1933a) The system Ca_2SiO_4-Fe_2SiO_4. American Journal of Science, 25, 273–297.

Bowen, N.L., Schairer, J.F., and Posnjak, E. (1933b) The system CaO-FeO-SiO_2. American Journal of Science, 26, 193–284.

Brenker, F.E. and Krot, A.N. (2004) Late-stage, high-temperature processesing in the Allende meteorite: Record from Ca,Fe-rich silicate rims around dark inclusions. American Mineralogist, 89, 1280–1289.

Brown, G.E.J. (1982) Olivine and silicate spinels. In P.H. Ribbe, Ed., Orthosilicates, 5, 2nd edition, p. 275–381. Reviews in Mineralogy Mineralogical Society of America, Chantilly, Virginia.

Buchanan, P.C., Zolensky, M.E., and Reid, A.M. (1997) Petrology of Allende dark inclusions. Geochimica et Cosmochimica Acta, 61, 1733–1743.

Cheng, W. and Greenwood, H.J. (1990) Topological construction of nets in ternary (n+3)-phase multisystems, with application to Al_2O_3-SiO_2-H_2O and MgO-SiO_2-H_2O. Canadian Mineralogist, 28, 305–320.

Cosca, M.A., Essene, E.J., Geissman, J.W., Simmons, W.B., and Coates, D.A. (1989) Pyrometamorphic rocks associated with naturally burned coal beds, Powder River Basin, Wyoming. American Mineralogist, 74, 85–100.

Davidson, P.M. and Lindsley, D.H. (1989) Thermodynamic analysis of pyroxene-olivine-quartz equilibria in the system CaO-MgO-FeO-SiO_2. American Mineralogist, 74, 18–30.

Davidson, P.M. and Mukhopadhyay, D.K. (1984) Ca-Fe-Mg olivines: phase relations and a solution model. Contributions to Mineralogy and Petrology, 86, 256–263.

Guo, Q. and Wang, S. (1988) The stability of laihunite—A thermodynamic reanalysis. Scientia China (Series B), XXXI, 1515–1528.

Gustafson, W.I. (1974) The stability of andradite, hedenbergite and related minerals in the system Ca-Fe-Si-O-H. Journal of Petrology, 15, 455–496.

Hillert, M. (2008) Phase Equilibria, Phase Diagrams and Phase Transformations—Their Thermodynamic Basis, p. 155–157. Cambridge University Press, U.K.

Hirschmann, M. (1991) Thermodynamics of multicomponent olivines and the solution properties of $(Ni,Mg,Fe)_2SiO_4$ and $(Ca,Mg,Fe)_2SiO_4$ olivines. American Mineralogist, 76, 1232–1248.

Holland, T.J.B. and Powell, R. (1998) An internally consistent thermodynamic data set for phases of petrological interest. Journal of Metamorphic Geology, 16, 309–343.

Hu, J.W., Yin, H.A., and Tang, M.L. (2000) A simple, universal theory and method for computer-plotting of phase diagrams of a multisystem—SFM method. Science in China Series B, Chemistry, 43, 219–224.

Johnson, R.E. and Muan, A. (1967) Activity-composition relations in solid solutions of the system CaO-"FeO"-SiO_2 in contact with metallic iron at 1080 °C. Transactions of the Metallurgical Society of AIME, 239, 1931–1939.

Kawasaki, T. (1998a) Effects of pressure and Ca^{2+} on the Fe-Mg partitioning between olivine and clinopyroxene. Review of High Pressure Science and Technology, 7, 95–97.

——— (1998b) Thermodynamic formulations of $(Ca,Fe,Mg)_2SiO_4$ olivine. Mineralogical Journal, 20, 135–149.

——— (1999) Thermodynamic analysis of partitioning of Ca, Fe and Mg between olivine and clinopyroxene. Geochemical Journal, 33, 33–58.

——— (2001) Experimental investigation of mixing properties of $(Ca,Fe,Mg)_2SiO_4$ olivine: Fe-Mg exchange with Ca-rich clinopyroxene and phase relations in olivine quadrilateral. Journal of Mineralogical and Petrological Sciences, 96, 217–242.

Kojima, T. and Tomeoka, K. (1996) Indicators of aqueous alteration and thermal metamorphism on the CV parent body: Microtextures of a dark inclusion from Allende. Geochimica et Cosmochimica Acta, 60, 2651–2666.

Korzhinskii, D.S. (1959) Physicochemical basis of the analysis of the paragenesis of minerals (Translated from Russian). 142 p. Consultants Bureau Inc., New York.

——— (1966) On thermodynamics of open systems and the phase rule (A reply to D.F. Weill and W.S. Fyfe). Geochimica et Cosmochimica Acta, 30, 829–835.

Krot, A.N., Scott, B.A., and Zolensky, M.E. (1997) Origin of fayalitic olivine rims and lath-shaped matrix olivine in the CV3 chondrite Allende and its dark inclusions. Meteoritics and Planetary Science, 32, 31–49.

Krot, A.N., Petaev, M.I., Zolensky, M.E., Keil, K., Scott, E.R.D., and Nakamura, K. (1998a) Secondary calcium-iron-rich minerals in the Bali-like and Allende-like oxidized CV3 chondrites and Allende dark inclusions. Meteoritics and Planetary Science, 33, 623–645.

Krot, A.N., Petaev, M.I., Scott, E.R.D., Choi, B., Zolensky, M.E., and Keil, K. (1998b) Progressive alteration in CV3 chondrites: More evidence for asteroidal alteration. Meteoritics and Planetary Science, 33, 1065–1085.

Krot, A.N., Brearley, A.J., Petaev, M.I., Kallemeyn, G.W., Sears, D.W.G., Benoit, P.H., Hutcheon, I.D., Zolensky, M.E., and Keil, K. (2000) Evidence for in situ growth of fayalite and hedenbergite in MacAlpine Hills 88107, ungrouped carbonaceous chondrite related to CM-CO clan. Meteoritics and Planetary Science, 35, 1365–1387.

Kurat, G., Varela, M.E., Brandstätter, F., Weckwerth, G., Clayton, R.N., Weber, H.W., Schultz, L., Wäsch, E., and Nazarov, M.A. (2004) D'Orbigny: A non-igneous angritic achondrite? Geochimica et Cosmochimica Acta, 68, 1901–1921.

Larsen, L.M. (1976) Clinopyroxenes and coexisting mafic minerals from the alkaline Ilimaussaq intrusion, South Greenland. Journal of Petrology, 17, 258–276.

Lépine, L., Provost, A., and Vielzeuf, D. (1992) Stability sequence along univariant lines in system of (C+N) phases. Comptes Rendus de l'Académie des Sciences de Paris, 314, 1463–1468.

Lindsley, D.H., Speidel, D.H., and Nafziger, R.H. (1968) P-T-f_{O_2} relations for the system Fe-O-SiO_2. American Journal of Science, 266, 342-360.

Liu, X.W. and Jin, Z.M. (2006) Microstructural features of ultrahigh-pressure garnet-peridotite from the Donghai district in the Sulu terrane: New evidence of rapid exhumation. Acta Geologica Sinica, 22, 1810–1816.

Liu, X.W., Jin, Z.M., Qu, J., and Wang, L. (2005) Exsolution of ilmenite and Cr-Ti magnetite from olivine of garnet-wehrlite. Science in China Series D, Earth Sciences, 48, 1368–1376.

Lottermoser, B.G. (2002) Mobilization of heavy metals from historical smelting slag dumps, north Queensland, Australia. Mineralogical Magazine, 66, 475–490.

Markl, G., Marks, M., and Wirth, R. (2001a) The influence of T, a_{SiO_2}, and f_{O_2} on exsolution textures in Fe-Mg olivine: An example from augite syenites of the Ilimaussaq Intrusion, South Greenland. American Mineralogist, 86, 36–46.

Markl, G., Marks, M., Schwinn, G., and Sommer, H. (2001b) Phase equilibrium constraints on intensive crystallization parameters of the Ilimaussaq complex, South Greenland. Journal of Petrology, 42, 2231–2258.

Mikouchi, T., Takeda, H., Miyamoto, M., Ohsumi, K., and McKay, G.A. (1995) Exsolution lamellae of kirschsteinite in magnesium-iron olivine from an angrite meteorite. American Mineralogist, 80, 585–592.

Mikouchi, T., Yamada, I., and Miyamoto, M. (2000) Symplectic exsolution in olivine from the Nakhla Martian meteorite. Meteoritics and Planetary Science, 35, 937–942.

Morse, S.A. (1980) Kiglapait mineralogy II: Fe-Ti oxide minerals and the activities of oxygen and silica. Journal of Petrology, 21, 685–719.

Moseley, D. (1984) Symplectic exsolution in olivine. American Mineralogist, 69, 139–153.

Mukhopadhyay, D.K. and Lindsley, D.H. (1983) Phase relations in the join kirschsteinite ($CaFeSiO_4$)-fayalite (Fe_2SiO_4). American Mineralogist, 68, 1089–1094.

Novikova, S.A. (2009) Fayalite from Fe-rich paralavas of ancient coal fires in the Kuzbass, Russia. Geology of Ore Deposits, 51, 800–811.

Ren, Y., Chen, F., Yang, J., and Gao, Y. (2008) Exsolutions of diopside and magnetite in olivine from mantle dunite, Luobusa ophiolite, Tibet, China. Acta Geologica Sinica, 82, 377–384.
Sautter, V., Jambon, A., and Boudouma, O. (2006) Cl-amphibole in the nakhlite MIL 03346: Evidence for sediment contamination in a Martian meteorite. Earth and Planetary Science Letters, 252, 45–55.
Schreinemakers, F.A.H. (1915–1925) In-, Mono-, and Divariant Equilibria, 348 p. Proceedings of Koninklijke Akademie van Wetentschappen te Amsterdam (English edition, 29 separate articles in the series).
Selleby, M. (1997) An assessment of the Ca-Fe-O-Si system. Metallurgical and Materials Transactions B, 28, 577–596.
Sokol, E., Sharygin, V., Kalugin, V., Volkova, N., and Nigmatulina, E. (2002) Fayalite and kirschsteinite solid solutions in melts from burned spoil-heaps, South Urals, Russia. European Journal of Mineralogy, 14, 795–807.
Stout, J.H. and Guo, Q. (1994) Phase diagram topology and the intrinsic stability rule. American Journal of Science, 294, 337–360.
Thompson, J.B.J. (1970) Geochemical reaction and open systems. Geochimica et Cosmochimica Acta, 34, 529–551.
Usdansky, S.I. (1983) BALSEQ: A BASIC program to balance and sequence reactions about invariant points. Computers and Geosciences, 9, 329–344.
Vielzeuf, D. and Boivin, P. (1984) An algorithm for the construction of petrogenetic grids: Application to some equilibria in granulitic paragneisses. American Journal of Science, 284, 760–791.
Xue, Y.X. (2008) Exsolved magnetite and clinopyroxene in olivine from Haladala gabbro, west Tianshan, NW China. Geochimica et Cosmochimica Acta, 72, A1048.
Zen, E.-A. (1966) Construction of pressure-temperature diagrams for multicomponent systems after the method of Schreinemakers: A geometric approach. U.S. Geological Survey Bulletin, 1225, 1–56.
Zhang, R.Y., Shu, J.F., Mao, H.K., and Liou, J.G. (1999) Magnetite lamellae in olivine and clinohumite from Dabie UHP ultramafic rocks, central China. American Mineralogist, 84, 564–569.
Zolensky, M.E., Krot, A.N., and Benedix, G. (2008) Record of low-temperature alteration in asteroids. In G.J. MacPherson, Ed., Oxygen in the Solar System, 68, p. 429–462. Reviews in Mineralogy and Geochemistry, Mineralogical Society of America, Chantilly, Virginia.
Zolotov, M.Y., Mironenko, M.V., and Shock, E.L. (2006) Thermodynamic constraints on fayalite formation on parent bodies of chondrites. Meteoritics and Planetary Science, 41, 1775–1796.

Manuscript received March 7, 2010
Manuscript accepted November 11, 2010
Manuscript handled by Rhian Jones